

Role of surface reflectivity in coherent backscattering measurements

P. M. Saulnier* and G. H. Watson

Department of Physics and Astronomy, University of Delaware, Newark, Delaware 19716

Received January 30, 1992

Surface reflectivity effects on coherent backscattering have been studied by using variable-reflectivity mirrors at the sample surface. Photon-transport parameters obtained from coherent backscattering were found to be significantly improved by using current theoretical models for samples with high surface reflectivity.

A resurgence of interest in light-scattering measurements from highly multiple-scattering random media has developed from the pursuit of photon localization. Recently the effects of surface reflections on photon-transport measurements in disordered systems have been considered.¹⁻⁴ Reflection from the sample surface of a photon attempting to escape a random medium has the effect of relaunching it and thereby increasing the average path length of photons injected into the sample. Photon-transport measurements that are sensitive to the total photon path are thus influenced by the presence of strong surface reflectivity, which is typically encountered for the large incidence angles abundant after multiple scatterings. The severity of this effect was first noticed in the optical memory effect and in large part accounted for discrepancy with existing theory.¹ Subsequent theoretical research considered the effects of surface reflections on coherent backscattering (CBS), pulse transmission, and frequency- and time-dependent speckle correlations.²⁻⁴ The experimental consequences of surface reflectivity have recently been demonstrated on angular correlation functions.⁴ The magnitude of these effects on coherent backscattering and their influence on transport parameter determination are reported here for observations in the presence of strong surface reflections.

Experiments on photon localization began with observations of CBS^{5,6} that arose from constructive interference between a wave and its time-reversed conjugate after scattering through a phase-conserving path. CBS is observed as an enhancement of scattered intensity in a narrow cone along the backscattering direction, comparable in intensity with that of the accompanying incoherent scattering, with an angular width inversely proportional to the magnitude of the photon wave vector k and the transport mean-free path length l^* . The reduction of the diffusion coefficient that results, inversely proportional to $(kl^*)^2$ in three dimensions, is known as weak localization; contributions to weak localization occur from all closed paths having lengths shorter than the inelastic (phase-breaking) length.

The phase difference associated with a multiply scattered path relative to its conjugate path is $\Delta\phi = (\mathbf{k}_i + \mathbf{k}_f) \cdot \mathbf{R}$, where $\mathbf{k}_{i,f}$ are the initial and final photon wave vectors and \mathbf{R} is the separation between the initial and final scatterers. In the diffusion approximation, the rms distance between first and last scatterers is $\mathcal{R} \sim \sqrt{sl^*}$ for path lengths s . For elastic multiple backscattering, phase coherence will be maintained (small $\Delta\phi$) within an angle given by $\theta_c k \sqrt{sl^*} < 1$. Longer paths thus predominantly contribute to CBS within much smaller angles than for low-order scattering. Broadening of CBS cones has been reported for paths terminated by absorption and by finite sample size.⁷ Surface reflectivity, which serves to reinject photons into the random medium, lengthens the average photon path and results in a narrowing of the CBS cone.

Photon transport in aqueous suspensions of monodisperse colloidal polystyrene spheres has been well studied by coherent backscattering^{8,9} and pulse transmission.^{10,11} These polyball suspensions also provide an ideal system for this study owing to their low absorptivity, well-controlled and well-characterized scattering parameters, and self-averaging properties. Polyball suspensions of diameters 0.135, 0.966, and 2.01 μm were studied at a nominal 10% volume fraction.

CBS measurements were made in a standard 45° beam-splitter geometry⁸ using a polarized 5-mW He-Ne laser and photon counting. A quarter-wave plate and a linear polarizer were used in front of the sample as shown in the inset of Fig. 1 to eliminate single scattering and to select the helicity-preserving part of the multiply scattered intensity in the backscattering direction.⁷ The CBS peak shape calculated for scalar waves has been shown to be in good quantitative agreement with helicity-preserving CBS for vector waves such as light.¹² This experimental configuration facilitates comparison with the scalar wave calculations of Refs. 2 and 3.

Surface reflectivity was varied by enclosing the suspension in cells constructed of various partially silvered mirrors. Mirrors were used that had normal reflectivities in air of 0.10, 0.25, 0.36, and 0.46, which dropped considerably when they were in con-

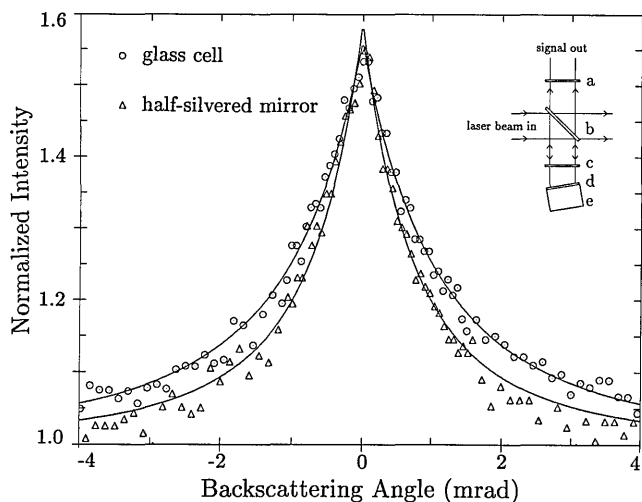


Fig. 1. CBS cone narrowing with increased surface reflectivity. The actual angular range was ± 8 mrad (reduced here for clarity). The sample was $2.01\text{-}\mu\text{m}$ polystyrene balls, 10% volume fraction in water. The inset shows the experimental geometry used: a, linear polarizer; b, beam splitter; c, quarter-wave plate; d, partially silvered mirror; e, sample cell.

tact with the aqueous polyball suspension. When averaged over all incidence angles and both polarization states, using a standard treatment¹³ for a silver mirror with a thin titania overcoat in contact with water, the effective surface reflectivities r were calculated and returned to 0.15, 0.30, 0.40, and 0.48, respectively. Reflections into the sample from the exterior glass-air interface were limited to $\sim 30^\circ$ from normal by geometrical constraint, over which the reflectivity averaged over both polarizations does not deviate significantly from 0.04.

The decrease in CBS cone widths arising from increased surface reflectivity is evident in Fig. 1, where the width is seen to drop by $\sim 25\%$ on changing from a glass cell to one with a half-silvered mirror. Previous studies have determined that the FWHM is $\sim 0.7/(kl^*)$ in a glass cell.⁸ Thus elevated surface reflectivity clearly leads to overestimates in l^* determined from CBS measurements. The CBS peaks were well fit by the following equations, derived for the case of no surface reflectivity from Refs. 8 and 14:

$$\gamma_0 = \frac{1}{(1 + 2z_0)} \frac{1}{(\alpha + v)^2 + u^2} \times \left\{ \frac{1}{v} + \frac{1}{\alpha} [1 - \exp(-2\alpha z_0)] \right\},$$

$$u = kl^*(1 - \cos \theta),$$

$$v = (1 + \sec \theta)/2,$$

$$\alpha = kl^*|\sin \theta|, \quad (1)$$

where $z_0 = 0.7104$ is the location of the trapping plane used in the diffusion model. Slight cone rounding owing to sample absorption, finite sample size, and finite angular resolution did not significantly impair the fitting procedure. The resulting kl^* parameters, indicated by the open symbols in

Fig. 2, increase with increasing reflectivity. The parameters for the three ball sizes have been normalized by the average value of kl^* as determined below.

Corrections to CBS from surface reflections were first considered through evaluation of the Green function for the case of finite reflectivity in the context of scalar diffusion.² Previous evaluation of CBS line shapes based on diffusion relied on the simplifying assumption of $r = 0$ with Dirichlet boundary conditions accompanied by placement of a trapping plane at a distance $0.7104l^*$ outside the sample surface.¹⁴ Surface reflectivity introduces mixed-type boundary conditions, complicating the evaluation of the Green function and necessitating reevaluation of z_0 for each value of r selected. Legendijk *et al.*² have proposed the following model for incorporating surface reflectivity into CBS:

$$\gamma_\epsilon(\theta) = \frac{1}{1 + 2(\epsilon + z_0)} \frac{1}{(\alpha + v)^2 + u^2} \times \left\{ \frac{1}{v} + \frac{1}{\alpha} \left[1 + \frac{\epsilon\alpha - 1}{\epsilon\alpha + 1} \exp(-2\alpha z_0) \right] \right\}, \quad (2)$$

where the reflectivity factor ϵ is related to the average surface reflectivity by $\epsilon = r/(1 - r)$. The transport parameters extracted from the experimental CBS peaks by using this model, with $z_0 = 0.7104$ throughout, are shown as the filled symbols in Fig. 2. Clearly this model accounts for the surface reflectivity, and the transport parameter extracted from each cone remains constant, within the experimental noise, as the reflectivity is increased.

An alternative approach for incorporating surface reflectivity, which circumvents the issue of associated boundary conditions, has been based on the

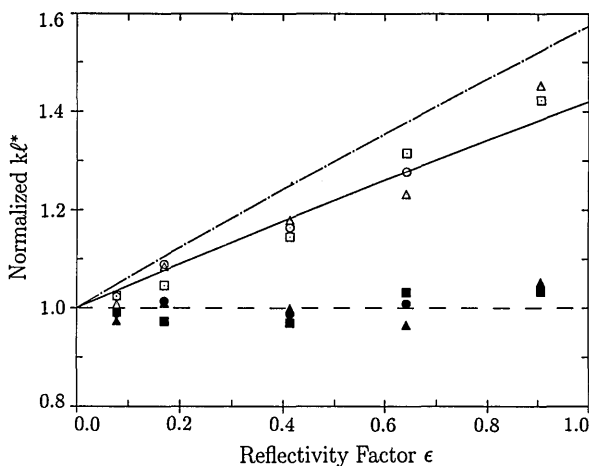


Fig. 2. Effects of surface reflectivity on transport parameter kl^* obtained from CBS with $0.135\text{-}\mu\text{m}$ (squares), $0.966\text{-}\mu\text{m}$ (circles), and $2.01\text{-}\mu\text{m}$ (triangles) balls. The open symbols indicate the rising value of kl^* obtained from Eqs. (1), where surface reflectivity is ignored; the relatively flat filled symbols result when surface reflectivity is incorporated by using Eq. (2). The solid curve shows the model of Ref. 2; the dashed curve shows the model of Ref. 3.

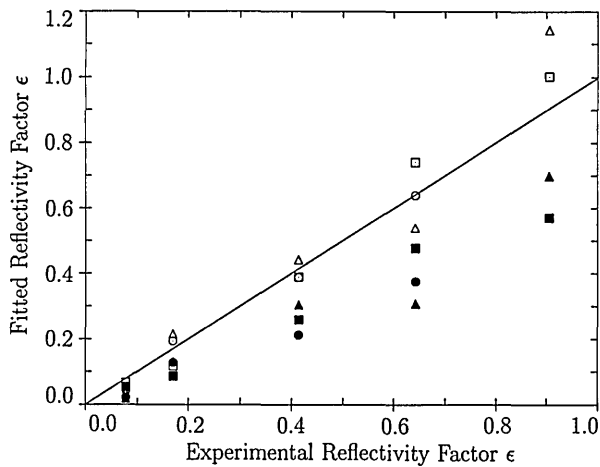


Fig. 3. Comparison of fitted reflectivity factors with 0.135- μm (squares), 0.966- μm (circles), and 2.01- μm (triangles) balls. The open symbols represent the values of ϵ extracted from the experimental coherent backscattering peak shapes using the model of Ref. 2; the filled symbols were obtained from the model of Ref. 3. The solid curve represents what would be perfect agreement between fitted and experimental values of angle-averaged reflectivities.

idea of treating reflection as a simple reinjection of light.³ An important advantage gained is that a closed-form expression emerges based on the $r = 0$ results obtained previously. For CBS, the $r = 0$ cone shape γ_0 is modified in Ref. 3 to

$$\gamma = (1 - r)\gamma_0 / (1 - r\gamma_0). \quad (3)$$

The solid and dashed curves in Fig. 2 represent the values that would result from ignoring surface reflectivity, according to the two models above, Eqs. (2) and (3), respectively. These curves were constructed by evaluating each model at a given reflectivity and then by fitting Eqs. (1) to it, extracting the value of kl^* that would be assigned were surface reflectivity ignored. Since the three resulting peak shapes are nearly identical, this procedure works surprisingly well. The model of Ref. 2 provides the best agreement with our observations, deviating somewhat at higher reflectivity, possibly owing to the failure of $z_0 = 0.7104$ to represent the boundary condition accurately. We were unable to fit successfully the model for CBS presented in Ref. 4.

Representing our results differently, Fig. 3 shows the value of the reflectivity factor assigned by least-

squares fitting of Eqs. (2) and (3) to the experimental peak shapes. The model of Ref. 2 again provides values for the reflectivity parameter ϵ in best agreement with the experimental values. The reflectivity parameter extracted by means of Eq. (3) is systematically low by approximately 40%.

In summary, surface-reflectivity effects on coherent backscattering measurements have been studied by using variable-reflectivity mirrors at the sample surface. We found that the model introduced by Lagendijk *et al.*² provides the best agreement with the experimental observations. Photon-transport determinations based on coherent backscattering can now be significantly improved for samples with high surface reflectivity.

We are pleased to acknowledge the support of the Petroleum Research Fund, administered by the American Chemical Society.

*Present address, Department of Physics, Carroll College, Waukesha, Wisconsin 53186.

References

1. I. Freund, M. Rosenbluh, and R. Berkovits, *Phys. Rev. B* **39**, 12403 (1989).
2. A. Lagendijk, R. Vreeker, and P. DeVries, *Phys. Lett. A* **136**, 81 (1989).
3. I. Freund and R. Berkovits, *Phys. Rev. B* **41**, 496 (1990).
4. J. X. Zhu, D. J. Pine, and D. A. Weitz, *Phys. Rev. A* **44**, 3948 (1991).
5. M. P. van Albada and A. Lagendijk, *Phys. Rev. Lett.* **55**, 2692 (1985).
6. P. E. Wolf and G. Maret, *Phys. Rev. Lett.* **55**, 2696 (1985).
7. S. Etamad, R. Thompson, M. J. Andrejco, S. John, and F. C. MacKintosh, *Phys. Rev. Lett.* **59**, 1420 (1987).
8. M. B. van der Mark, M. P. van Albada, and A. Lagendijk, *Phys. Rev. B* **37**, 3575 (1988).
9. P. E. Wolf, G. Maret, E. Akkermans, and R. Maynard, *J. Phys. (Paris)* **49**, 63 (1988).
10. G. H. Watson, P. A. Fleury, and S. L. McCall, *Phys. Rev. Lett.* **58**, 945 (1987).
11. P. M. Saulnier, M. P. Zinkin, and G. H. Watson, *Phys. Rev. B* **42**, 2621 (1990).
12. F. C. MacKintosh and S. John, *Phys. Rev. B* **37**, 1884 (1988).
13. M. Born and E. Wolf, *Principles of Optics*, 6th ed. (Pergamon, Oxford, 1980).
14. E. Akkermans, P. E. Wolf, and R. Maynard, *Phys. Rev. Lett.* **56**, 1471 (1986).